



American Society of Hematology  
 2021 L Street NW, Suite 900,  
 Washington, DC 20036  
 Phone: 202-776-0544 | Fax 202-776-0545  
 editorial@hematology.org

## Inhibition of a new AXL isoform (AXL3) induces apoptosis of mantle cell lymphoma cells

Tracking no: BLD-2022-015581R3

Pascal Gelebart (University of Bergen, Norway) May Gjerstad (University of Bergen, Norway) Susanne Benjaminsen (University of Bergen, Norway) Jianhua Han (University of Bergen, Norway) Ida Karlsen (University of Bergen, Norway) Mireia Mayoral Safont (University of Bergen, ) Calum Leitch (University of Bergen, Norway) Zinayida Fandalyuk (University of Bergen, Norway) Mihaela Popa (University of Bergen, ) Lars Helgeland (Haukeland University Hospital, Norway) Bela Papp (INSERM, U976, France) Fanny Baran-Marszak (Institut National de la Santé et de la Recherche Médicale (INSERM) U978, France) Emmet McCormack (University of Bergen, Norway)

### Abstract:

Mantle cell lymphoma (MCL) is an aggressive B-cell non-Hodgkin lymphoma having a poor overall survival that is in need for the development of new therapeutics. In this study, we report the identification and expression of a new isoform splice variant of the tyrosine kinase receptor AXL in MCL cells. This new AXL isoform, called AXL3, lacks the ligand-binding domain of the commonly described AXL splice variants and is constitutively activated in MCL cells. Interestingly, functional characterization of AXL3, using CRISPRi, revealed that only the knockdown of this isoform leads to apoptosis of MCL cells. Importantly, pharmacological inhibition of AXL activity resulted in a significant decrease in the activation of well-known pro-proliferative and survival pathways activated in MCL cells (i.e. b-catenin, AKT, and NF- $\kappa$ B). Therapeutically, pre-clinical studies using a xenograft mouse model of MCL indicated that bemcentinib is more effective than ibrutinib in reducing the tumour burden and to increase the overall survival. Our study highlights the importance of a previously unidentified AXL splice variant in cancer and the potential of bemcentinib as a targeted therapy for MCL.

**Conflict of interest:** No COI declared

**COI notes:**

**Preprint server:** No;

**Author contributions and disclosures:** P.G., M.E.G., and E.M.C. designed the experiments, P.G., M.E.G., S.B., J.H., I.K., Z.F. and M.P. performed all the experimental procedures, P.G., M.E.G., I.K. and E.M.C. analysed the data. L.H., B.P. and F.B.M. provided MCL patients. P.G., M.E.G., I.K. and E.M.C. wrote the paper.

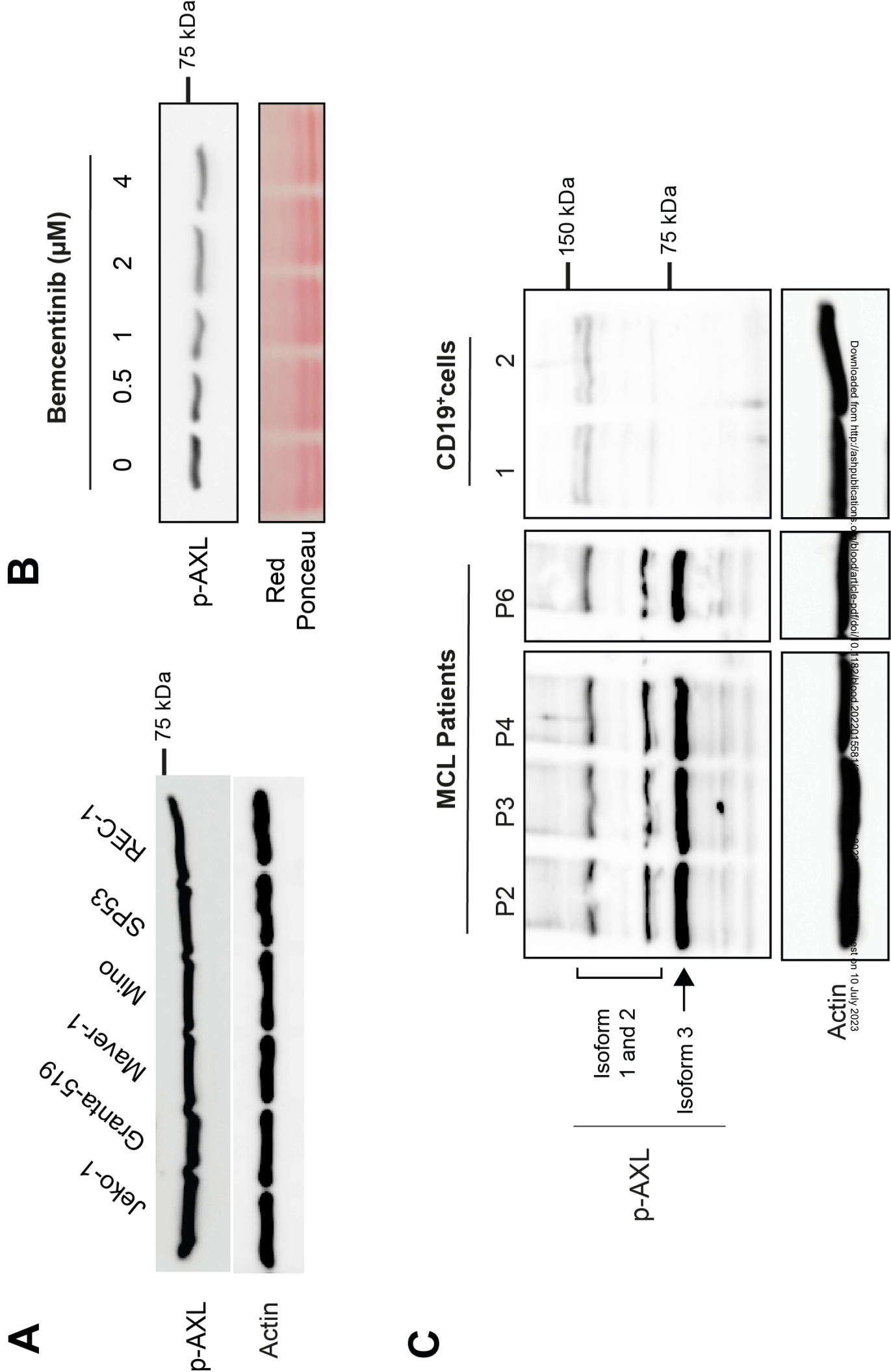
**Non-author contributions and disclosures:** No;

**Agreement to Share Publication-Related Data and Data Sharing Statement:** Supplemental Data and Methods can be found in a supplement material available with the online version of this article. For original data, please contact the corresponding author.

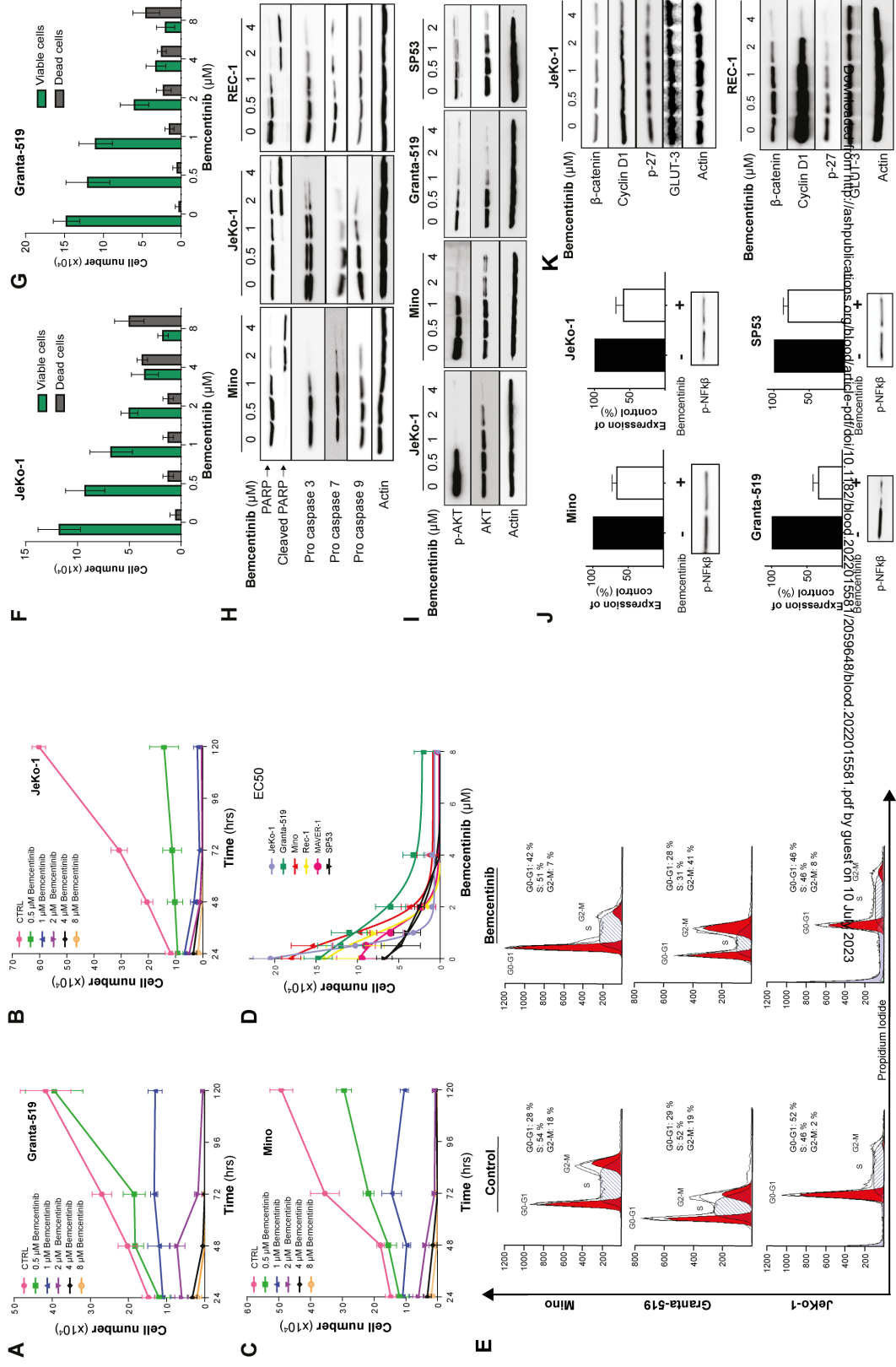
**Clinical trial registration information (if any):**

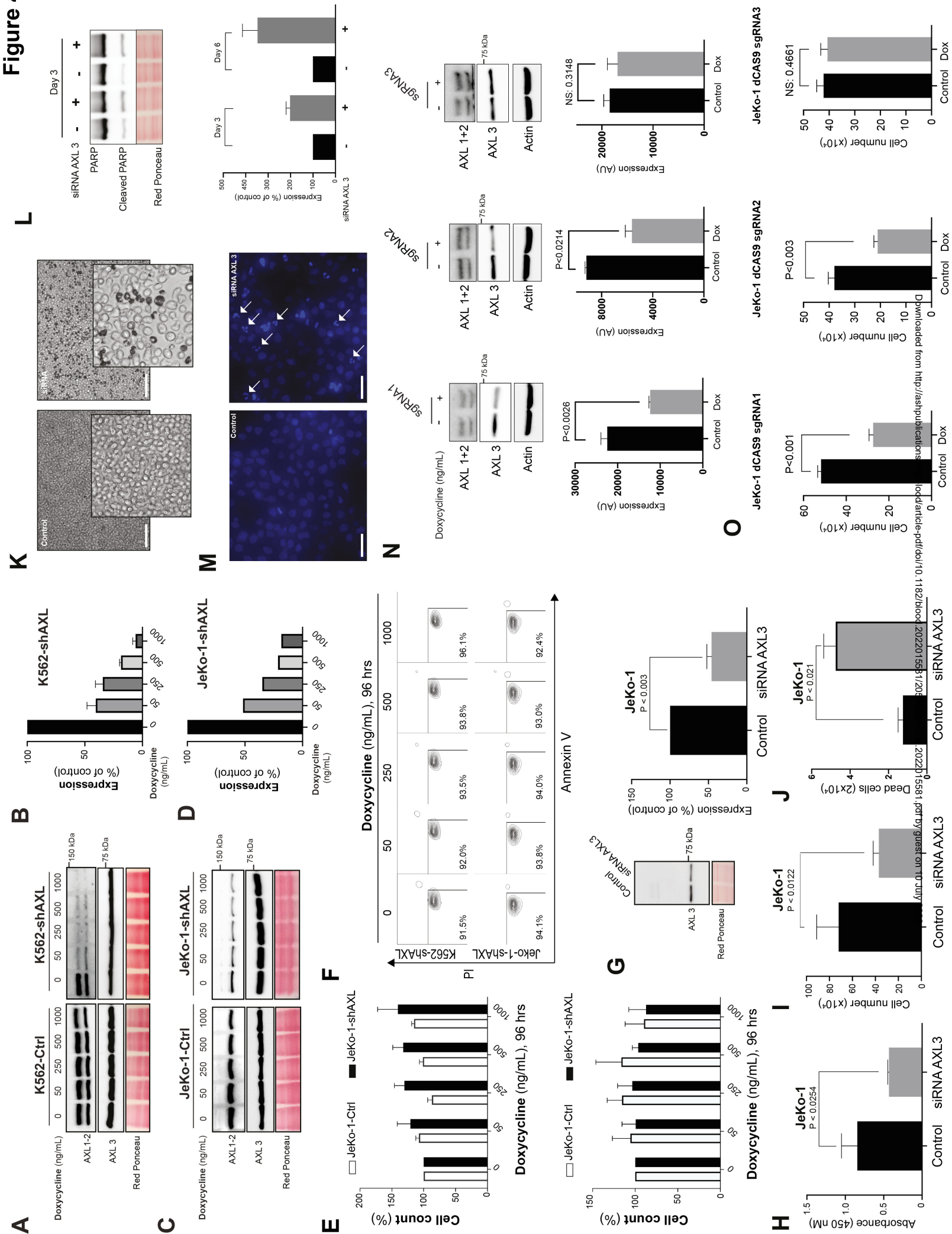


**Figure 2**

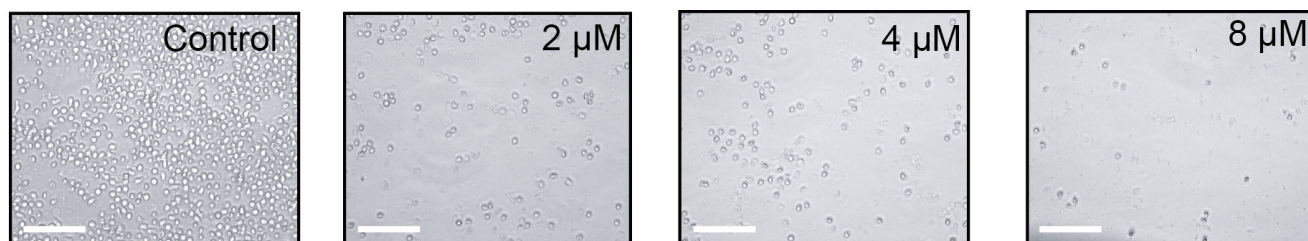
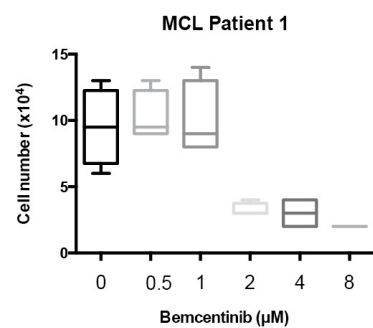
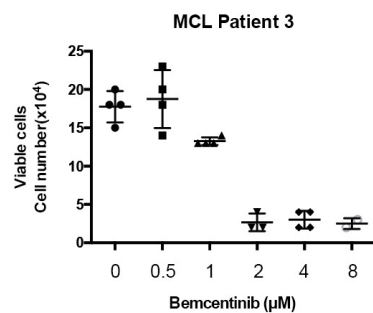
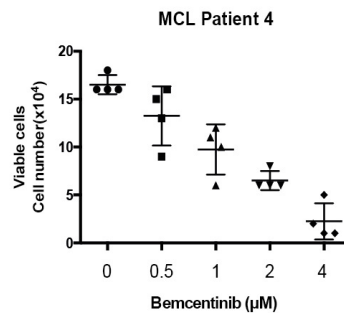
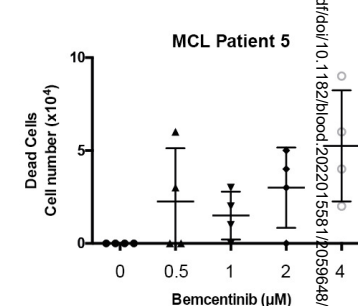
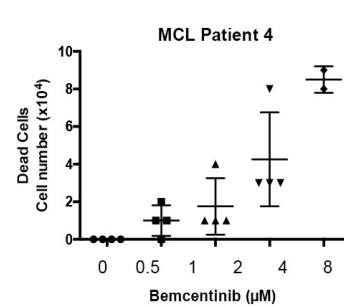
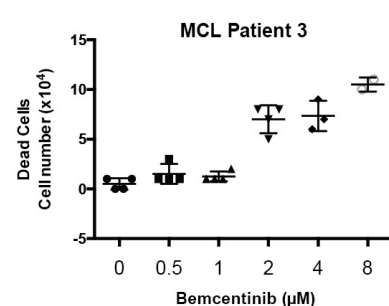
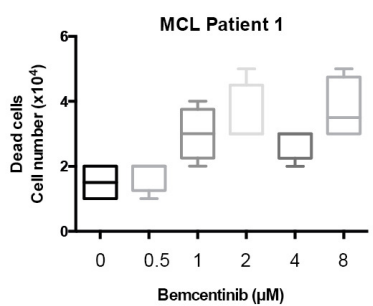
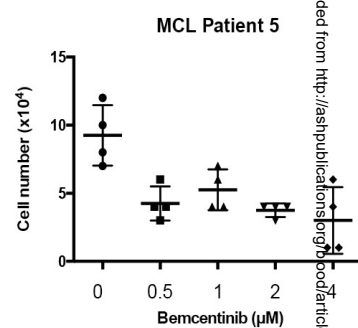
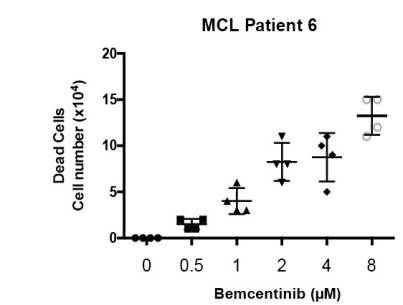
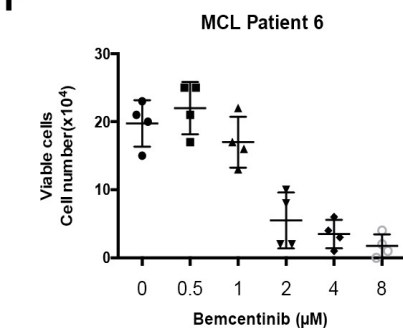
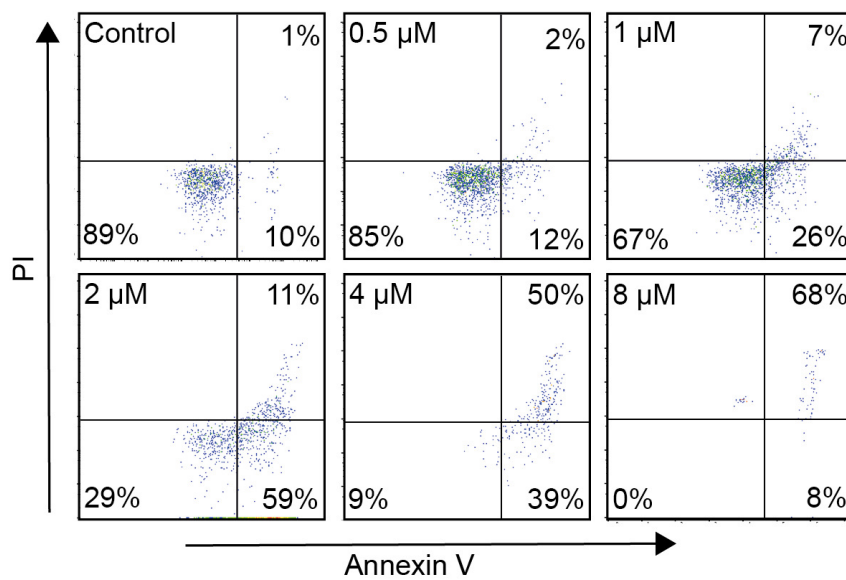


**Figure 3**

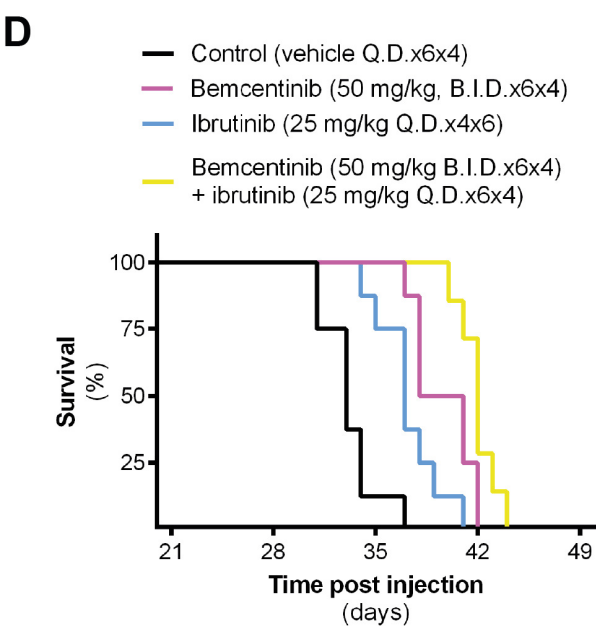
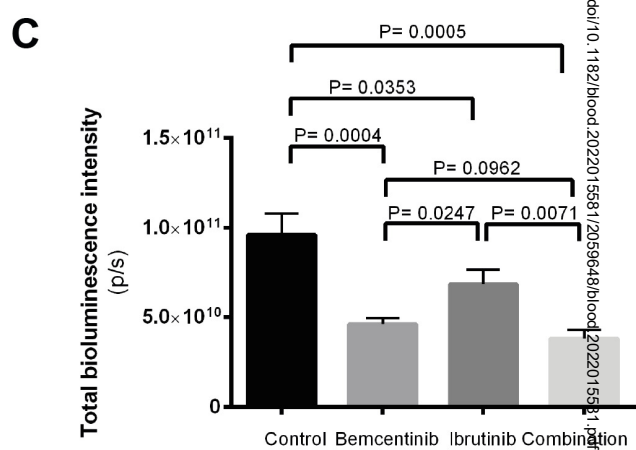
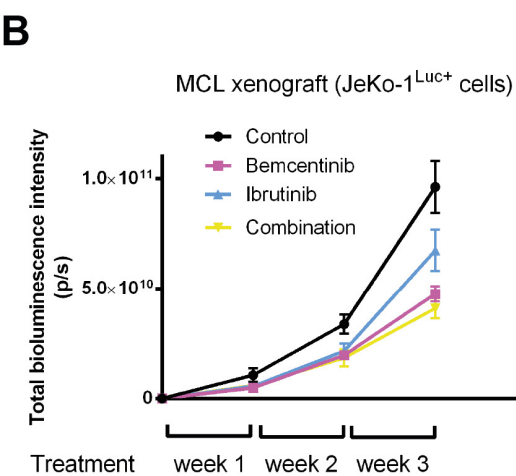
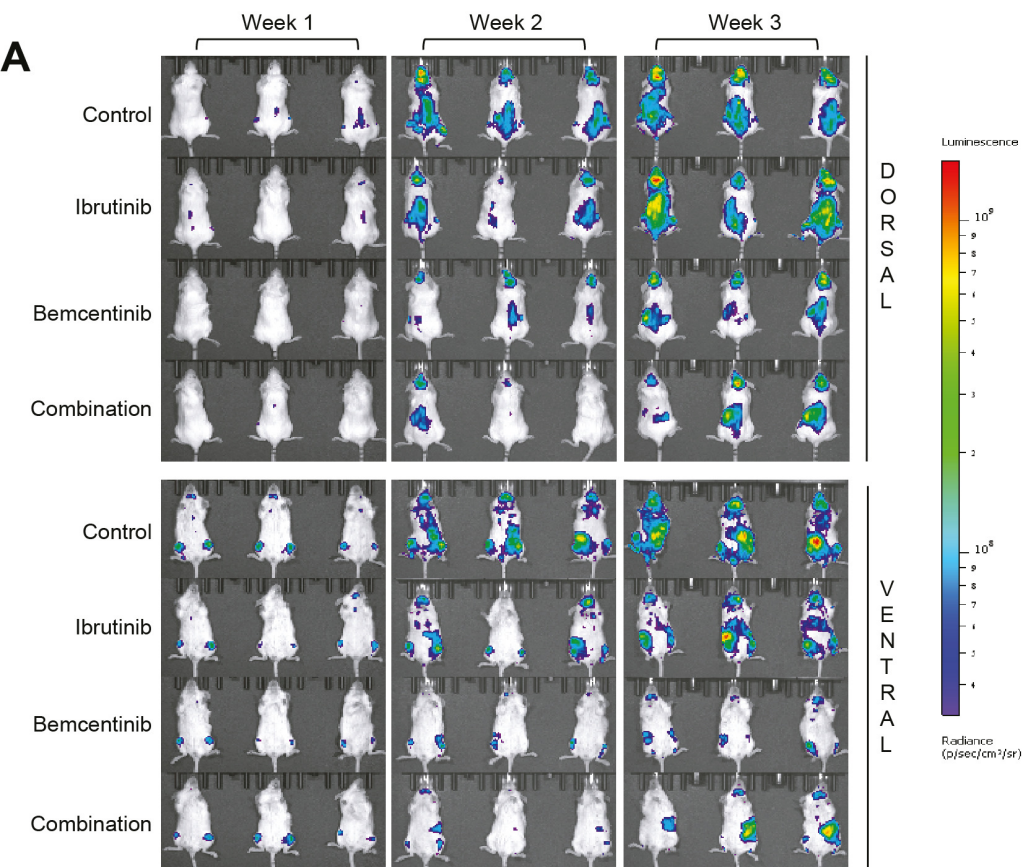


**Figure 4**



**Figure 5****A****B****C****D****E****F****G**

# Figure 6



Control vs Bemcentinib P=0.001  
Control vs Ibrutinib P=0.0207  
Control vs Combination P=0.0001  
Bemcentinib vs Ibrutinib P=0.0347  
Combination vs Bemcentinib P= 0.0361  
Combination vs Ibrutinib P= 0.0006





34 Sequence 2 : GenBank OR103211

35 Sequence 3 : GenBank OR103212

36 Sequence 4 : GenBank OR103213

37

38

39

40

41 **Running Title:** New AXL isoform inactivation induces MCL apoptosis.

42 **Key words:** AXL isoform 3, bemcentinib, apoptosis, pre-clinical studies, mantle cell  
43 lymphoma.

44 **Abstract:** 175 words; **Main Text:** 4550 words.

45 **Figure:** 6. **Supplemental figure:** 11

46 **References:** 60

#### 47 **Abstract**

48

49 Mantle cell lymphoma (MCL) is an aggressive B-cell non-Hodgkin lymphoma having  
50 a poor overall survival that is in need for the development of new therapeutics. In this  
51 study, we report the identification and expression of a new isoform splice variant of  
52 the tyrosine kinase receptor AXL in MCL cells. This new AXL isoform, called AXL3,  
53 lacks the ligand-binding domain of the commonly described AXL splice variants and  
54 is constitutively activated in MCL cells. Interestingly, functional characterization of  
55 AXL3, using CRISPRi, revealed that only the knockdown of this isoform leads to  
56 apoptosis of MCL cells. Importantly, pharmacological inhibition of AXL activity  
57 resulted in a significant decrease in the activation of well-known pro-proliferative and  
58 survival pathways activated in MCL cells (i.e.  $\beta$ -catenin, AKT, and NF- $\kappa$ B).

59 Therapeutically, pre-clinical studies using a xenograft mouse model of MCL indicated  
60 that bemcentinib is more effective than ibrutinib in reducing the tumour burden and to  
61 increase the overall survival. Our study highlights the importance of a previously  
62 unidentified AXL splice variant in cancer and the potential of bemcentinib as a  
63 targeted therapy for MCL.

64

#### 65 **Key Points**

- 66 • The newly identified AXL3 isoform is aberrantly expressed and represents a  
67 new biomarker and therapeutic target for MCL.

68

69 In a pre-clinical model of MCL, inhibition of AXL tyrosine kinase, using  
70 bemcentinib, shows superior activity than ibrutinib.

71

72

73

74

75

## 76 Introduction

77 Mantle cell lymphoma (MCL) is an aggressive type of B-cell non-Hodgkin's  
78 lymphoma (NHL) that originates from mature B-cells. MCL represents between 5 to 7  
79 % of all NHL<sup>1-5</sup>. Clinical management of MCL remains a significant challenge. While  
80 current therapeutic options include several regimens of conventional chemotherapy,  
81 most patients will relapse, highlighting the need for more efficient molecularly  
82 targeted therapeutics specific for this disease. One of the characteristic features of  
83 MCL is the recurrent chromosomal translocation, t(11;14)(q13;q32) that brings the  
84 cyclin D1 gene under the control of the enhancer of the immunoglobulin heavy chain  
85 gene (IgH), leading to the overexpression of the cyclin D1 protein which in turn leads  
86 to a deregulation of the G<sub>1</sub>/S phase transition in the cell cycle<sup>6</sup>. Cyclin D1 abnormal  
87 overexpression of was initially thought to be the primary driver of the disease.  
88 However, it was demonstrated that additional defects in many other cellular  
89 processes, such as those involved in cell survival and proliferation (WNT/ $\beta$ -catenin  
90<sup>7,8</sup>, NF- $\kappa$ B<sup>9,10</sup>, AKT<sup>11</sup>, IL22RA1<sup>12</sup>, apoptosis, DNA repair<sup>13</sup>), in addition to  
91 contributions from the tumour microenvironment<sup>14,15</sup> are also required. More  
92 recently, the aberrant expression of the transcription factor SOX11 has been  
93 identified to be involved in the regulation of MCL cell growth<sup>16,17</sup>. Additionally, BCR  
94 expression, which is crucial for normal B-cell function, has been demonstrated to be  
95 constitutively activated in MCL development<sup>18</sup>. Importantly, ibrutinib monotherapy  
96 targeting the tyrosine kinase BTK, which is constitutively activated in MCL, has been  
97 shown to achieve an overall response rate (ORR) of 68 % ( $n = 111$ ) in  
98 refractory/relapsed MCL patients in phase II clinical trial<sup>19</sup>. The median duration of  
99 response was around 17.5 months<sup>19,20</sup>. Clinical studies evaluating ibrutinib as a  
100 single agent<sup>21</sup> or in combination with other agents, such as rituximab, resulted in an  
101 ORR of 87 % ( $n = 50$ ). More recently, emerging new therapies were investigated in  
102 MCL<sup>22,23</sup>. Next generation of BTK inhibitors Acalabrutinib, Zanubrutinib and  
103 pirtobrutinib have all been evaluated in MCL, with Pirtobrutinib demonstrating  
104 encouraging results in refractory B- cell malignancies, including MCL<sup>24</sup>. On the of  
105 immunotherapy front, CAR T cells targeting CD19 have demonstrated durable  
106 remission in relapse and refractory MCL patients<sup>25</sup>. Although these results highlight  
107 the potential of molecularly targeted approaches and immunotherapy (CAR T/BiTes),

108 those treatments are non-curative and resultingly, novel therapeutic modalities are  
109 still urgently required for this disease <sup>20,26,27</sup>.

110

111 The receptor tyrosine kinase (RTK) AXL belongs to the TAM family of receptors <sup>28,29</sup>.  
112 This small family of RTKs shares the same overall structure and together they  
113 regulate and contribute to a wide array of signalling pathways leading to cellular  
114 responses such as survival, proliferation, and migration <sup>30,31</sup>. According to The  
115 Human Protein Atlas<sup>32</sup>, AXL is ubiquitously expressed in the human body but not  
116 detected in lymphoid tissue. Its expression in normal B-cells is assumed to be absent  
117 at the mRNA and protein level <sup>33,34</sup>. The vitamin K-dependent protein growth arrest-  
118 specific protein 6 (Gas6) <sup>35</sup> is the principal ligand of AXL. The AXL receptor can also  
119 be activated through ligand-independent homodimerization and heterodimerization  
120 with a non-TAM receptor, such as EGFR <sup>36</sup>. AXL signalling is transduced through  
121 PI3K-AKT-mTOR, MEK-ERK, NF- $\kappa$ B and JAK/STAT activation <sup>37</sup>. Interestingly, *Axl*  
122 was first discovered and cloned from chronic myeloid leukaemia cells following  
123 blastic transformation where it was identified as a transforming gene <sup>28,29</sup>. AXL was  
124 described to have oncogenic activity in a variety of solid tumours (breast and lung  
125 cancer, melanoma and glioma) <sup>28,31,34,37</sup>, and several forms of leukaemia (acute  
126 myeloid leukaemia, chronic lymphocytic leukaemia) <sup>33,38</sup>. AXL expression was  
127 associated with poor prognosis and outcome in AML <sup>38</sup> and has been demonstrated  
128 to be a driver of invasiveness, migration and of therapeutic resistance in cancer cells  
129 <sup>37</sup>. AXL has also been linked to the epithelial-to-mesenchymal transition (EMT) in  
130 breast cancer and non-small cell lung carcinoma (NSCLC) <sup>37,39,40</sup>. Interestingly,  
131 although AXL expression was investigated in most haematological malignancies <sup>29</sup>, it  
132 has never been examined in MCL.

133

134 In this study, we investigate whether AXL could constitute a therapeutic target in  
135 MCL. We first demonstrate that AXL is expressed and activated in MCL. We then  
136 provide evidence for the existence of a third AXL isoform and its role in the survival  
137 of MCL cells. Moreover, we demonstrate the efficacy of bemcentinib, as a single  
138 agent or in combination, in a newly developed MCL xenograft model providing a  
139 translational basis for clinical implementation of AXL inhibition in MCL as a novel  
140 therapeutic strategy.

## 141 **Methods**

142

143 The study was performed in accordance with the Declaration of Helsinki, and all  
144 samples, were collected following written informed consent. All patients were above  
145 16 years of age. The biobank and the clinical protocols were approved by the ethical  
146 committee at the Haukeland University Hospital, Bergen, Norway (Ethical approval  
147 REK Vest 2012/2245) and Avicenne Hospital HUPSSD, Paris, France.

148

149 Details of procedures can be found in the Supplemental Methods section.

150

### 151 **Cell culture and patient samples**

152 The MCL cell lines (JeKo-1, SP53, REC-1, Mino, Granta-519) previously described  
153 in the following study<sup>7</sup> were used. The MCL cell line Maver-1 was a gift from Dr.  
154 Alberto Zamò (University of Verona, Italy). The CML cell line K562, and the ductal  
155 pancreatic adenocarcinoma cell line MIA-PaCa-2 were purchased from DSMZ  
156 (Braunschweig, Germany), while the Phoenix-AMPHO cells were kindly provided by  
157 BergenBio AS (Bergen, Norway).

158

### 159 **Establishment of an inducible AXL shRNA knockdown system**

160 To investigate the role of AXL in MCL, a short hairpin RNA (shRNA) conditional  
161 knockdown approach was employed. The CML cell line K562 was used as a positive  
162 control. To transduce JeKo-1 and K562 cells with the vector of interest, retrovirus  
163 was made using Phoenix-AMPHO cells.

164

### 165 **Generation of inducible sgRNA CRISPRi cell lines**

166 All plasmids used in the CRISPRi experiment were bought from Addgene  
167 (Watertown, MA, USA) unless otherwise stated. JeKo-1 cells were first transduced  
168 with Lenti-dCas9-KRAB-blast (plasmid #89567). dCas9 positivity was done by  
169 western blotting like previously described using an anti-Cas9 monoclonal antibody  
170 (Prod nr. 10C11-A12, ThermoFisher Scientific). Positive cells were then transduced  
171 with a FgHtUTG (plasmid #70183) plasmid cloned with sgRNA sequences targeting  
172 AXL3. The cells were named JeKo-1 dCas9 sgRNA1, JeKo-1 dCas9 sgRNA2 and  
173 JeKo-1 dCas9 sgRNA3.



174 **sgRNA design and cloning into the inducible sgRNA expression vector**

175 The CRISPRi sgRNA sequences were designed using the designer tool CRISPR-  
176 ERA Version 1.2: using an input of 1500 bp upstream of TSS and 1500 bp  
177 downstream of the TSS of AXL3 transcript (<http://www.ncbi.nlm.nih.gov/>).

178 ***In vivo* evaluation of bemcentinib in an MCL mouse xenograft model**

179 The lentiviruses, RediFect Red-FLuc-GFP, were purchased from PerkinElmer Inc.  
180 (Waltham, MA, USA) and used to transduce the JeKo-1 cells and generate the JeKo-  
181 1<sup>Luc+</sup> cells that contain GFP and Luciferase reporter. All the animal experimentations  
182 were approved by the Norwegian Animal Research Authority and performed  
183 according to the European Convention for the protection of vertebrates used for  
184 scientific purposes.

185

186 **Results**

187 **AXL is expressed in MCL cell lines and primary MCL cells**

188 To investigate the presence of AXL in MCL, we first demonstrated the expression of  
189 AXL transcript using RT-PCR. Primers were specifically designed to amplify AXL  
190 isoform 1 and 3 based on the exon structure released in public database (NCBI)  
191 (**Figure 1A, Figure S1A**). However, since the AXL isoform 2 differs only by a 27 bp  
192 internal exon, the primer set named AXL1-2 is also able to amplify AXL isoform 1  
193 and 2. RNA extracted from five MCL cell lines was used, and the results are  
194 illustrated in **Figure 1B**. AXL mRNA was detectable in the MCL cell lines examined.  
195 MIA-PaCa-2 and K562 cells served as positive controls. We detected AXL protein  
196 expression in MCL cell lines using western blotting. As AXL is a heavily glycosylated  
197 protein, we used two different antibodies with distinct binding sites to avoid false  
198 negative detection of AXL. One antibody targeting the N-terminal part of the protein  
199 (labelled N-ter) and the other one recognizes the C-terminal part of the AXL protein  
200 (labelled C-ter). As shown in **Figure 1C**, the C-terminal antibody can recognize AXL  
201 at its expected molecular weight in MIA-PaCa-2 cells (around 98 kDa), as well as the  
202 glycosylated form at 120-140 kDa. However, in all MCL cells, this antibody  
203 recognizes a band corresponding to the expected size of AXL3 (around 70 kDa).  
204 This isoform can also be detected in K562 and MIA-PaCa-2 but at a lower level of  
205 expression than in MCL cells. In contrast, the AXL N-ter antibody can identify AXL  
206 expression at a size of around 120-140 kDa in all the cell lines tested (**Figure 1D**).  
207 Flow cytometry was used to evaluate the expression of AXL in MCL cell lines. As  
208 demonstrated in **Figure 1E**, the Jeko-1 MCL cell line showed an increased signal in  
209 comparison to the isotype control. K562 cells served as the positive control in this  
210 experiment. We then assessed the expression of AXL in primary MCL patient cells at  
211 both mRNA and protein level. As shown in **Figure 1F**, the different AXL transcripts  
212 can be detected in MCL patient samples. Furthermore, using either the AXL N-ter or  
213 C-ter antibodies, AXL protein expression can be detected in MCL primary cells  
214 (**Figure 1G and H**) and is overexpressed in comparison to PBMCs or CD19<sup>+</sup> cells.  
215 To confirm that MCL expresses the AXL3 transcript we cloned the full cDNA  
216 transcript including the 5' and 3' UTR parts from JeKo-1 and K562 cells (Ensemble  
217 database: putative AXL-203 transcript ID: ENST00000593513.1, 2557 base pair). As  
218 shown in **Figure 1I**, the amplification product using the primer to clone the AXL3

219 transcript (**Supplemental Figure 1B**) led to the amplification of products at the  
220 expected size. The full product was cloned, and the alignment of the sequencing  
221 result confirmed the presence and identity of the AXL3 transcript with the predicted  
222 exon structure (**Figure 1J and K**). We also cloned part of the AXL1 messenger  
223 excluding a portion of the untranslated 3' messenger part. The full amplification  
224 product was also clone and confirmed the existence of AXL1 transcript in MCL cells  
225 (Ensemble database: AXL-201 transcript ID: ENST00000301178.9, 4717 base pair).  
226

### 227 **AXL is constitutively activated in MCL cell lines and primary MCL cells**

228 To investigate the level of AXL activation in MCL cell lines and MCL primary cells,  
229 we examined its phosphorylation status by western-blot using an antibody specific  
230 for phosphorylated AXL (p-AXL). As shown in **Figure 2A**, AXL phosphorylation can  
231 be detected in all MCL cell lines with bands corresponding to the expected molecular  
232 weight of AXL3. To confirm the specificity of the detected AXL phosphorylation, the  
233 MCL cell line JeKo-1 was treated with increasing doses of the AXL inhibitor,  
234 bemcentinib. As described in **Figure 2B**, the AXL inhibitor induced a significant  
235 decrease in the phosphorylation status of AXL. AXL phosphorylation was also  
236 evaluated in MCL primary patient cells (**Figure 2C**), demonstrating AXL  
237 phosphorylation. Both in MCL cell lines and patient cells, the strongest AXL  
238 phosphorylation was detected for the band corresponding to the third isoform of AXL.  
239 CD19<sup>+</sup> cells demonstrated some weak p-AXL staining for AXL isoform 1-2 in  
240 comparison to MCL cells (**Figure 2C**). We also evaluated the expression of GAS6,  
241 the ligand of AXL, in MCL cells. As shown in **Figure S2A**, the GAS6 transcript can  
242 be detected in all MCL cell lines. However, no GAS6 protein expression can be  
243 detected in the supernatant of MCL cell culture medium (**Figure S2B**). Together,  
244 these observations indicate that the newly described AXL3 protein is the major AXL  
245 isoform activated in MCL cells, and this is supported by the observation that the  
246 known ligand of AXL is not expressed at the protein level in MCL cell lines, and no p-  
247 AXL1 and 2 isoforms can be detected.

248

### 249 **Pharmacologic inhibition of AXL activity by bemcentinib induces significant 250 cell-growth inhibition and apoptosis of MCL cell lines**

251 To determine the biological importance of AXL in MCL cells, we inhibited AXL  
252 activation in MCL cell lines using the most potent pharmacological inhibitor described

253 so far, bemcentinib<sup>41</sup>. To show that bemcentinib can bind AXL in vivo we used the  
254 cellular thermal shift assay (CETSA) (**Figure S3**). To determine the EC<sub>50</sub> of  
255 bemcentinib on MCL cell lines, the MCL cells were treated with a wide range of drug  
256 concentrations. As shown in **Figure 3**, bemcentinib induced a significant reduction in  
257 the number of cells in a time and dose-dependent manner (**Figure 3A, B and C**). At  
258 48 hours post-treatment, the EC<sub>50</sub> values were in the range of 1 to 2 µM for most of  
259 the MCL cell lines (**Figure 3D**) with SP53 being the most sensitive cell line and  
260 Maver-1 the least sensitive (**Figure 3D**). As illustrated in **Figure 3E**, cell cycle  
261 analysis revealed that bemcentinib induces cell cycle arrest either in the G1 phase,  
262 for the Mino cells, or at the G2 phase for the Granta-519 and JeKo-1 MCL cells.  
263 Next, we investigated whether bemcentinib induced apoptosis in MCL cells. As  
264 shown in **Figure 3F and G**, bemcentinib treatment of various MCL cell lines for 48  
265 hours leads to an increase in trypan blue positive cells. Moreover, a dose-dependent  
266 cleavage of PARP, as well as proteolytic activation of pro-caspases 3, 7 and 9 can  
267 be observed after bemcentinib treatment (**Figure 3H**). We also found that increasing  
268 concentrations of bemcentinib induced a dose-dependent decrease in AKT (**Figure**  
269 **3I**) and NF-κB activation (**Figure 3J**). Furthermore, we also evaluated the biological  
270 effect of bemcentinib on other pathways known to be dysregulated in MCL. As  
271 shown in **Figure 3K**, bemcentinib induced a decrease in the expression of cyclin D1,  
272 p27 and of β-catenin. Taken together, these results demonstrate that major  
273 signalling pathways involved in the survival and proliferation of MCL cells are  
274 inhibited by the inhibition of AXL activation.

275

### 276 **Knockdown of the AXL 3 isoform induces apoptosis of MCL cells**

277 To further investigate the role of AXL in MCL, we used a conditional shRNA  
278 approach. The MCL cell line JeKo-1 and the CML cell line K562 were transduced  
279 with the inducible AXL shRNA or control shRNA vector containing the mCherry  
280 reporter vector. As shown in **Figure S4A and B**, an mCherry fluorescence signal,  
281 indicating the presence of the inducible construct, is observed in the different  
282 transduced cell lines. AXL knockdown was induced by adding different  
283 concentrations of doxycycline (ranging from 0 to 1000 nM; **Figure 4A and C**). The  
284 knockdown efficiency was analysed by Western blotting, and a 90% decrease of  
285 AXL1 and 2 can be observed in the two different models (**Figure 4B and D and S4C**

286 **and D**). In contrast, no decrease in AXL protein was observed in the control cells  
287 (**Figure 4A and C - Left panel**). Interestingly, the level of AXL3 expression is not  
288 effected by the increased concentrations of doxycycline in the K562 transduced cell  
289 line. Similarly, a decrease in protein expression of AXL1 and AXL2 can be observed  
290 in JeKo-1-shAXL cells after addition of doxycycline. However, as seen in the K562  
291 cells, AXL3 expression remains unaltered. To evaluate the effect of decreased AXL  
292 expression on cell growth and viability we used the trypan blue assay. Surprisingly,  
293 no statistical difference in total cell number was observed between the different  
294 doxycycline concentrations in any of the transduced cell lines (**Figure 4E**). Moreover,  
295 the control and the shRNA-AXL cell lines present no statistical difference in total cell  
296 number after 96 hrs of doxycycline treatment. Annexin V/PI flow cytometry was  
297 performed to further evaluate the impact of AXL1 and AXL2 knockdown on cell  
298 viability. After 96 hrs of doxycycline treatment, cells were stained and run on the flow  
299 cytometer and no statistical differences in the number of apoptotic cells were  
300 observed for the different concentrations of doxycycline used (**Figure 4F**). All cell  
301 lines were approximately 90% viable after 96 hrs exposure to 1000 nM doxycycline.  
302 To further evaluate the biological significance of AXL in MCL, we investigated the  
303 role of AXL3 on MCL biology. AXL3 expression was downregulated using a siRNA  
304 approach and we assessed the effects on cell growth and apoptosis on MCL cells.  
305 As shown in **Figure 4G**, siRNA specifically targeting AXL3 (**Figure S5A**) induced a  
306 substantial reduction in AXL3 protein expression of approximately 50% within 72  
307 hours of transfection. Blockade of AXL3 expression using siRNA significantly  
308 decreased cell growth by approximately 50% at 5 days post-transfection as  
309 determined by WST-1 assay (**Figure 4H**) and cell count (**Figure 4I, Figure S5B**).  
310 Moreover, bright-field optical microscope imaging revealed the presence of dead  
311 cells in cells transfected with the AXL3 siRNA (**Figure 4J and K**). As shown in  
312 **Figure 4L**, inhibition of AXL3 expression by siRNA in JeKo-1 cells induced the  
313 cleavage of PARP. Moreover, Hoechst staining (**Figure 4M**) clearly demonstrated  
314 formation of apoptotic bodies with condensed and fragmented nuclei. These results  
315 underline that, in contrast to the AXL1 and 2 isoforms, only the specific  
316 downregulation of AXL3 protein expression has an impact on MCL cell growth and  
317 viability. Since the design of specific AXL3 siRNA needed to target the 5' UTR  
318 sequence of the AXL3 mRNA and prevented us to find multiple suitable effective  
319 siRNA sequences, we decided to validate our siRNA observations using an CRISPRi



320 approach. To this end, JeKo-1 cells were made positive for dCAS9 expression  
321 (**Figure S6 A, B and C**) and we designed three sgRNAs targeting the AXL3  
322 promoter (**Figure S6D**). As shown in **Figure 4N (Left and middle panel)**, two of the  
323 sgRNAs targeting the AXL3 lead to a decrease in AXL3 protein expression. This was  
324 accompanied by a decrease in the cell proliferation (**Figure 4O**). In contrast, no  
325 effect on cell proliferation was observed in control cells (**Figure S6E**) or cells  
326 carrying the sgRNA that failed to decrease AXL3 expression (**Figure 4N and O -**  
327 **right panel**).

328

### 329 **Bemcentinib induces cells death of primary MCL cells *in vitro***

330 To further evaluate the efficacy of bemcentinib on MCL cells, we treated primary  
331 MCL cells with various concentrations of bemcentinib (**Figure 5A**). Bemcentinib  
332 induced a significant dose-dependent reduction in cell growth, as well as a decrease  
333 in cell viability, as determined by trypan blue staining (**Figure 5B, C, D, E and F**).  
334 This result is further supported by the Annexin V/PI staining which shows an  
335 increase in cell death after treatment with bemcentinib (**Figure 5G**). As observed for  
336 the MCL cell lines, the EC<sub>50</sub> of bemcentinib is around 1.5  $\mu$ M in MCL primary cells  
337 (**Figure 5B, C, D, E and F**). Moreover, we also demonstrate synergy between  
338 bemcentinib and ibrutinib *in vitro* (**Supplemental Figure 7**). Overall, these results  
339 indicate that MCL primary cells are sensitive to bemcentinib *in vitro*.

340

### 341 **Bemcentinib shows superior efficacy than ibrutinib to decrease MCL tumour 342 burden and enhances the overall survival**

343 To investigate whether pharmacological targeting of AXL could potentially benefit  
344 patients, we used our newly developed orthotopic JeKo-1 xenograft mouse model of  
345 MCL (**Figure S8A-F**). The *in vivo* efficacy of bemcentinib, ibrutinib and the  
346 combination of the two drugs was evaluated. As shown in **Figure 6A**, the disease  
347 develops in the bone marrow, spleen, femur and brain. BLI revealed that at week 3  
348 the control group had the highest average total bioluminescence signal, followed by  
349 the ibrutinib treatment group and the bemcentinib treatment group, respectively  
350 (**Figure 6B and C**). The bemcentinib treatment group demonstrated significantly  
351 lower total bioluminescence signal compared to the control group ( $p = 0,00004$ ;  
352 unpaired Student's t-test), while the ibrutinib treatment group also showed  
353 statistically significant decrease in total bioluminescence in comparison to the control

354 group ( $p = 0.0353$ ; unpaired student's t-test). In addition, the total bioluminescence  
355 signal of the bemcentinib treatment group was significantly lower than the ibrutinib  
356 treatment group ( $p = 0.0247$ ; student's unpaired t-test). The total bioluminescence of  
357 the combination group was also significantly lower than the control ( $p = 0.0005$ ;  
358 unpaired student's t-test) and ibrutinib group ( $p = 0.0071$ ; unpaired student's t-test).  
359 These results demonstrate that bemcentinib shows efficacy in a pre-clinical  
360 xenograft MCL mouse model. The combination of bemcentinib and ibrutinib  
361 demonstrates the highest overall survival (**Figure 6D**).

## 362 Discussion

363

364 AXL is a tyrosine kinase receptor involved in various biological processes such as  
365 stimulation of cell proliferation and regulation of the innate immune response<sup>42</sup>. Its  
366 role in the oncogenesis of several forms of solid cancers, including pancreatic<sup>43</sup>,  
367 ovarian<sup>44</sup> and breast carcinoma<sup>45</sup>, has been widely demonstrated. AXL expression  
368 has also been investigated in various forms of haematological malignancies.  
369 Neubauer *et al.*<sup>34</sup> found that the AXL transcript can be detected in several forms of  
370 leukaemia, including AML<sup>38,46</sup> and CLL<sup>33</sup>. However, AXL expression has never been  
371 reported in mantle cell lymphoma. In the present work, we demonstrate that AXL is  
372 expressed at the mRNA and protein level in MCL cell lines and patient cells.  
373 Interestingly, we have also demonstrated for the first time the existence of a third  
374 AXL isoform in MCL cells. To confirm the existence of the AXL3 mRNA we cloned  
375 the full transcript (**Figure 1**). Sequencing confirms that the exon structure of this  
376 messenger corresponds to the predicted AXL3 isoform. Despite the isoform being  
377 predicted and described in the Ensembl database, to our knowledge, no previous  
378 reports have cloned, identified, or studied the isoform in human cells. In contrast to  
379 the two well-characterized AXL1 and 2 isoforms, the third AXL protein presents a  
380 singular extracellular structure. The transcript encodes for a protein of 626 a.a.,  
381 which lacks the two Ig-like domains but retains the two-fibronectin type 3-like (FNIII)  
382 repeats. This configuration makes this isoform a peculiar AXL receptor as there is  
383 only one other type of tyrosine kinase family that possesses only extracellular  
384 fibronectin type 3 domains, the ROS tyrosine kinase family. Unlike AXL isoform 1  
385 and 2, GAS-6 will not bind and activate the AXL3 isoform. Instead, the ligand of the  
386 FNIII domain remains to be formally identified. Nevertheless, some studies seem to  
387 indicate that the fibronectin III domain can bind to integrin proteins<sup>47,48</sup>, indicating  
388 that AXL activation can be triggered by cell-cell contact or by interaction with the  
389 extracellular microenvironment. Moreover, we cannot exclude that this third isoform  
390 can also be activated by a ligand-independent mechanism or by heterodimerization  
391 with another receptor as it was previously reported for AXL1 and 2<sup>49</sup>. The AXL  
392 expression/activation pattern seems complex in MCL. We were able to detect GAS-6  
393 transcript in most MCL cell lines (Supplemental Figure S2), indicating that an  
394 autocrine activation cannot be ruled-out in MCL. These novel insights into the  
395 expression and activation of AXL isoforms may significantly impact therapeutic

396 strategies. Pharmaceutical attempts to block AXL activation by preventing GAS-6  
397 binding may be by-passed in cells expressing the AXL3 isoform. Splice variant  
398 switching, obtained by genetic mutation or other mechanisms, is now a well-  
399 established mechanism used by cancer cells to gain proliferation advantage or  
400 resistance to chemotherapy treatments<sup>50-52</sup>.

401

402 To further evaluate the impact of AXL inhibition in MCL cells we have used a  
403 conditional knockdown shRNA approach to decrease the expression of AXL. The  
404 shRNA construct was previously characterized to be effective in reducing AXL  
405 expression<sup>39</sup>. Interestingly, using this approach we were able to effectively shut-  
406 down AXL1 and 2 protein expression in the AXL shRNA JeKo-1 and AXL shRNA  
407 K562 cells. In both cell lines, the AXL3 protein expression was unaffected. Despite  
408 the ability of bemcentinib to induce cell death of wild-type JeKo-1 and K562 cells,  
409 neither cell proliferation, nor viability was affected by the knockdown of AXL1 and  
410 AXL2. (**Figure 4**). These results diverge from the reported findings of Ben-Batalla *et*  
411 *al.*<sup>38</sup>, that describe that silencing of AXL1-2 in CML cells resulted in a reduction of  
412 cell viability<sup>38</sup>. However, the authors have not evaluated the effect of the AXL  
413 knockdown on the AXL3 protein expression that may be responsible for the  
414 observed effect on cell viability. Nevertheless, our results are in accordance with  
415 Dufies *et al.*<sup>53</sup> and Gioia *et al.*<sup>54</sup>, who have shown that AXL1-2 knockdown doesn't  
416 induce cell apoptosis in CML. Moreover, a study performed in the squamous cell  
417 carcinoma line (MET1) also reported that knockdown of AXL1-2 did not affect cell  
418 proliferation<sup>55</sup> nor induce apoptosis. As shown in **Figure 1**, the AXL3 isoform, at the  
419 protein level, seems to be considerably more highly expressed than AXL 1 and 2 in  
420 MCL cell lines, as well as in the CML cell line K562. The observation that AXL3  
421 protein cannot be downregulated in our conditional shRNA system may be explained  
422 by the structure of the AXL3 mRNA. In fact, this isoform presents a long 5'UTR  
423 sequence that may be involved in the stabilization of the messenger. Moreover, it is  
424 also well-established that mRNAs can be regulated by post-secondary modifications,  
425 like N6-adenosine methylation, that can control mRNA decay as reported for SOX2  
426 or KLF4 mRNA<sup>56</sup>. Therefore, it is possible to consider that different AXL mRNAs  
427 may have different lifetimes and may be more or less sensitive to a particular RNAi  
428 sequence (shRNA or siRNA) used to induce the degradation of the AXL mRNA. To  
429 further evaluate the function of AXL3, we have custom designed a specific siRNA

430 targeting only AXL isoform 3. As shown in **Figure 4G**, with this approach we were  
431 able to decrease AXL3 protein expression that was observable at 72 hours (**Figure**  
432 **4G**). As shown in **Figure 4H, I, K, L and M**, the downregulation of AXL3 expression  
433 leads to the reduction of growth and apoptosis of MCL cells. To further characterize  
434 the function of AXL3, we took advantage of the fact that this isoform uses a different  
435 promoter than the previously described AXL isoforms, to selectively block the  
436 transcription of AXL3 by a CRISPRi approach. As illustrated in **Figure 4N**, induction  
437 of the sgRNA targeting the *Axl3* promoter leads to a decrease of AXL3 protein  
438 expression as well as to a significant decrease in cell proliferation. Interestingly, the  
439 time course of expression of AXL3 decrease was slower in the CRISPRi experiment  
440 than in the siRNA approach. However, this result is not unexpected as CRISPRi  
441 affects transcription rather than RNA degradation and are in accordance with  
442 previous reports using CRISPRi<sup>57,58</sup>. By using the CETSA, we were able to show  
443 that bemcentinib can bind the AXL3 isoform. Altogether these results indicate that  
444 the inhibition of the expression or activity of AXL3 is responsible for the growth  
445 inhibition and apoptosis of MCL cells.

446

447 Our *in vitro* data reveal that bemcentinib can reduce the proliferation and induces  
448 apoptosis of cells that were not killed by standard dose of ibrutinib (i.e. Granta-519,  
449 **Figure 3A and 3D**). This observation is of interest as it underlines that ibrutinib  
450 resistance can be overcome by blocking AXL activation. One-third of patients treated  
451 with ibrutinib alone relapse within 2 years of treatment<sup>26</sup>. It may therefore be  
452 valuable to investigate if a co-treatment of MCL cells with an AXL and a next  
453 generation of BTK inhibitor, like pirtobrutinib could be favourable. To support this  
454 concept, our study also provide evidence that inhibition of AXL activity, in conjunction  
455 with the BTK inhibitor ibrutinib, increases the overall survival of MCL-carrying mice in  
456 comparison to mice treated with either ibrutinib or bemcentinib alone. Moreover, it  
457 was previously shown that co-treatment can be beneficial for MCL patients with other  
458 drugs<sup>59,60</sup>. In this context, the development of new therapeutic modalities targeting  
459 simultaneously several vulnerabilities identified in MCL should be of interest for the  
460 development of multimodal therapy for the long-term remission or cure of MCL  
461 patient.

462 It is interesting to note that the AXL3 isoform can also be detected in other  
463 haematological (i.e. chronic myelogenous leukaemia) and solid (i.e. Pancreatic



464 ductal adenocarcinoma) malignancies, suggesting that AXL3 may also have broader  
465 implications for the aetiology of several cancer forms. In particular, the development  
466 of therapeutic antibodies targeting AXL in pancreatic, or breast cancer, have so far  
467 demonstrated a limited application. This may be explained, in part, by the inability of  
468 those antibodies to recognize and bind the new AXL3 isoform permitting tumour cell  
469 evasion by this therapeutic strategy.

470 In conclusion, we show that MCL cells express AXL and that it contributes to the  
471 biology of MCL by promoting cell growth and survival characteristics. We also  
472 discovered that MCL cells express a third AXL isoform that this is responsible for the  
473 cell growth and survival effect observed in MCL. Moreover, we also demonstrate, in  
474 a xenograft mouse model of MCL, that bemcentinib, an AXL inhibitor that got fast-  
475 track designation in Non-Small Cell Lung cancer and currently in clinical trials in  
476 acute myeloid leukaemia, may hold promise in treating MCL as a single agent or in  
477 combination with BTK inhibitors and/or immunotherapy modalities (CAR T/BiTes).

478

#### 479 **Acknowledgements**

480 This study was supported by research grants from the Research council of Norway  
481 (grant no. 326300, 327278) Norwegian cancer society (Kreftforeningen, grant  
482 number: 223171, 182735), the Helse Vest region (grant number: 911182) awarded  
483 to E.M.C. We would like to thank BergenBio AS for providing the bemcentinib  
484 compound and the shRNA constructs that were used for this study, as well as Brith  
485 Bergum from the Flow Cytometry Core facility at the University of Bergen for  
486 technical advice and support. We also would like to thank the Molecular Imaging  
487 Center core facility and vivarium at the University of Bergen for the help provided  
488 and Tine AS for product support.

#### 489 **Authorship Contributions**

490 P.G., M.E.G., and E.M.C. designed the experiments, P.G., M.E.G., S.B., J.H., I.K.,  
491 M.M.S, C.L., Z.F. and M.P. performed all the experimental procedures, P.G., M.E.G.,  
492 I.K. and E.M.C. analysed the data. L.H., B.P. and F.B.M. provided MCL patients.  
493 P.G., M.E.G., I.K. and E.M.C. wrote the paper.

494

#### 495 **Declaration of Conflicts of Interest**

496 The authors declare no competing interests and none of the authors have shares or  
497 received grants or financial support from BerGenBio AS.

498 **References**

- 499 1. Jares P, Colomer D, Campo E. Molecular pathogenesis of mantle cell  
500 lymphoma. *J Clin Invest.* 2012;122(10):3416-3423.
- 501 2. Jares P, Colomer D, Campo E. Genetic and molecular pathogenesis of  
502 mantle cell lymphoma: perspectives for new targeted therapeutics. *Nat Rev Cancer.*  
503 2007;7(10):750-762.
- 504 3. Kupperts R. Mechanisms of B-cell lymphoma pathogenesis. *Nat Rev Cancer.*  
505 2005;5(4):251-262.
- 506 4. Quintanilla-Martinez L. The 2016 updated WHO classification of lymphoid  
507 neoplasias. *Hematol Oncol.* 2017;35 Suppl 1:37-45.
- 508 5. Swerdlow SH, Campo E, Pileri SA, et al. The 2016 revision of the World  
509 Health Organization classification of lymphoid neoplasms. 2016;127(20):2375-2390.
- 510 6. Thelander EF, Rosenquist R. Molecular genetic characterization reveals new  
511 subsets of mantle cell lymphoma. *Leuk Lymphoma.* 2008;49(6):1042-1049.
- 512 7. Gelebart P, Anand M, Armanious H, et al. Constitutive activation of the Wnt  
513 canonical pathway in mantle cell lymphoma. *Blood.* 2008;112(13):5171-5179.
- 514 8. Lazarian G, Friedrich C, Quinquenel A, et al. Stabilization of beta-catenin  
515 upon B-cell receptor signaling promotes NF-kB target genes transcription in mantle  
516 cell lymphoma. *Oncogene.* 2020;39(14):2934-2947.
- 517 9. Balaji S, Ahmed M, Lorence E, Yan F, Nomie K, Wang M. NF-kappaB  
518 signaling and its relevance to the treatment of mantle cell lymphoma. *J Hematol*  
519 *Oncol.* 2018;11(1):83.
- 520 10. Rahal R, Frick M, Romero R, et al. Pharmacological and genomic profiling  
521 identifies NF-kappaB-targeted treatment strategies for mantle cell lymphoma. *Nat*  
522 *Med.* 2014;20(1):87-92.
- 523 11. Rudelius M, Pittaluga S, Nishizuka S, et al. Constitutive activation of Akt  
524 contributes to the pathogenesis and survival of mantle cell lymphoma. *Blood.*  
525 2006;108(5):1668-1676.
- 526 12. Gelebart P, Zak Z, Dien-Bard J, Anand M, Lai R. Interleukin 22 signaling  
527 promotes cell growth in mantle cell lymphoma. *Translational oncology.* 2011;4(1):9-  
528 19.
- 529 13. Camacho E, Hernandez L, Hernandez S, et al. ATM gene inactivation in  
530 mantle cell lymphoma mainly occurs by truncating mutations and missense  
531 mutations involving the phosphatidylinositol-3 kinase domain and is associated with  
532 increasing numbers of chromosomal imbalances. *Blood.* 2002;99(1):238-244.
- 533 14. Balsas P, Palomero J, Eguileor A, et al. SOX11 promotes tumor protective  
534 microenvironment interactions through CXCR4 and FAK regulation in mantle cell  
535 lymphoma. *Blood.* 2017;130(4):501-513.
- 536 15. Zhang L, Yang J, Qian J, et al. Role of the microenvironment in mantle cell  
537 lymphoma: IL-6 is an important survival factor for the tumor cells. *Blood.*  
538 2012;120(18):3783-3792.
- 539 16. Vegliante MC, Palomero J, Perez-Galan P, et al. SOX11 regulates PAX5  
540 expression and blocks terminal B-cell differentiation in aggressive mantle cell  
541 lymphoma. *Blood.* 2013;121(12):2175-2185.
- 542 17. Ferrando AA. SOX11 is a mantle cell lymphoma oncogene. *Blood.*  
543 2013;121(12):2169-2170.
- 544 18. Burger JA, Wiestner A. Targeting B cell receptor signalling in cancer:  
545 preclinical and clinical advances. *Nat Rev Cancer.* 2018;18(3):148-167.
- 546 19. Wang ML, Rule S, Martin P, et al. Targeting BTK with ibrutinib in relapsed or  
547 refractory mantle-cell lymphoma. *N Engl J Med.* 2013;369(6):507-516.

- 548 20. Wang ML, Blum KA, Martin P, et al. Long-term follow-up of MCL patients  
549 treated with single-agent ibrutinib: updated safety and efficacy results. *Blood*.  
550 2015;126(6):739-745.
- 551 21. Inamdar AA, Goy A, Ayoub NM, et al. Mantle cell lymphoma in the era of  
552 precision medicine-diagnosis, biomarkers and therapeutic agents. *Oncotarget*.  
553 2016;7(30):48692-48731.
- 554 22. Qualls D, Kumar A, Epstein-Peterson ZD. Targeting the immune  
555 microenvironment in mantle cell lymphoma: implications for current and emerging  
556 therapies. *Leuk Lymphoma*. 2022:1-13.
- 557 23. Hanel W, Epperla N. Emerging therapies in mantle cell lymphoma. *J Hematol*  
558 *Oncol*. 2020;13(1):79.
- 559 24. Mato AR, Shah NN, Jurczak W, et al. Pirtobrutinib in relapsed or refractory B-  
560 cell malignancies (BRUIN): a phase 1/2 study. *Lancet*. 2021;397(10277):892-901.
- 561 25. Wang M, Munoz J, Goy A, et al. KTE-X19 CAR T-Cell Therapy in Relapsed or  
562 Refractory Mantle-Cell Lymphoma. *N Engl J Med*. 2020;382(14):1331-1342.
- 563 26. Stephens DM, Spurgeon SE. Ibrutinib in mantle cell lymphoma patients: glass  
564 half full? Evidence and opinion. *Ther Adv Hematol*. 2015;6(5):242-252.
- 565 27. Cheah CY, Chihara D, Romaguera JE, et al. Patients with mantle cell  
566 lymphoma failing ibrutinib are unlikely to respond to salvage chemotherapy and have  
567 poor outcomes. *Ann Oncol*. 2015;26(6):1175-1179.
- 568 28. O'Bryan JP, Frye RA, Cogswell PC, et al. axl, a transforming gene isolated  
569 from primary human myeloid leukemia cells, encodes a novel receptor tyrosine  
570 kinase. *Mol Cell Biol*. 1991;11(10):5016-5031.
- 571 29. Neubauer A, O'Bryan JP, Fiebeler A, Schmidt C, Huhn D, Liu ET. Axl, a novel  
572 receptor tyrosine kinase isolated from chronic myelogenous leukemia. *Semin*  
573 *Hematol*. 1993;30(3 Suppl 3):34.
- 574 30. Linger RM, Keating AK, Earp HS, Graham DK. TAM receptor tyrosine  
575 kinases: biologic functions, signaling, and potential therapeutic targeting in human  
576 cancer. *Adv Cancer Res*. 2008;100:35-83.
- 577 31. Axelrod H, Pienta KJ. Axl as a mediator of cellular growth and survival.  
578 *Oncotarget*. 2014;5(19):8818-8852.
- 579 32. Uhlen M, Fagerberg L, Hallstrom BM, et al. Proteomics. Tissue-based map of  
580 the human proteome. *Science*. 2015;347(6220):1260419.
- 581 33. Ghosh AK, Secreto C, Boysen J, et al. The novel receptor tyrosine kinase Axl  
582 is constitutively active in B-cell chronic lymphocytic leukemia and acts as a docking  
583 site of nonreceptor kinases: implications for therapy. *Blood*. 2011;117(6):1928-1937.
- 584 34. Neubauer A, Fiebeler A, Graham DK, et al. Expression of axl, a transforming  
585 receptor tyrosine kinase, in normal and malignant hematopoiesis. *Blood*.  
586 1994;84(6):1931-1941.
- 587 35. Sasaki T, Knyazev PG, Clout NJ, et al. Structural basis for Gas6-Axl  
588 signalling. *Embo j*. 2006;25(1):80-87.
- 589 36. Vouri M, Croucher DR, Kennedy SP, An Q, Pilkington GJ, Hafizi S. Axl-EGFR  
590 receptor tyrosine kinase hetero-interaction provides EGFR with access to pro-  
591 invasive signalling in cancer cells. *Oncogenesis*. 2016;5(10):e266.
- 592 37. Gay CM, Balaji K, Byers LA. Giving AXL the axe: targeting AXL in human  
593 malignancy. *Br J Cancer*. 2017;116(4):415-423.
- 594 38. Ben-Batalla I, Schultze A, Wroblewski M, et al. Axl, a prognostic and  
595 therapeutic target in acute myeloid leukemia mediates paracrine crosstalk of  
596 leukemia cells with bone marrow stroma. *Blood*. 2013;122(14):2443-2452.

- 597 39. Gjerdrum C, Tiron C, Hoiby T, et al. Axl is an essential epithelial-to-  
598 mesenchymal transition-induced regulator of breast cancer metastasis and patient  
599 survival. *Proc Natl Acad Sci U S A*. 2010;107(3):1124-1129.
- 600 40. Byers LA, Diao L, Wang J, et al. An epithelial-mesenchymal transition gene  
601 signature predicts resistance to EGFR and PI3K inhibitors and identifies Axl as a  
602 therapeutic target for overcoming EGFR inhibitor resistance. *Clin Cancer Res*.  
603 2013;19(1):279-290.
- 604 41. Myers SH, Brunton VG, Unciti-Broceta A. AXL Inhibitors in Cancer: A  
605 Medicinal Chemistry Perspective. *J Med Chem*. 2016;59(8):3593-3608.
- 606 42. Lemke G. Biology of the TAM receptors. *Cold Spring Harb Perspect Biol*.  
607 2013;5(11):a009076.
- 608 43. Leconet W, Larbouret C, Chardes T, et al. Preclinical validation of AXL  
609 receptor as a target for antibody-based pancreatic cancer immunotherapy.  
610 *Oncogene*. 2014;33(47):5405-5414.
- 611 44. Huang RY, Antony J, Tan TZ, Tan DS. Targeting the AXL signaling pathway  
612 in ovarian cancer. *Mol Cell Oncol*. 2017;4(2):e1263716.
- 613 45. Leconet W, Chentouf M, du Manoir S, et al. Therapeutic Activity of Anti-AXL  
614 Antibody against Triple-Negative Breast Cancer Patient-Derived Xenografts and  
615 Metastasis. *Clin Cancer Res*. 2017;23(11):2806-2816.
- 616 46. Rochlitz C, Lohri A, Bacchi M, et al. Axl expression is associated with adverse  
617 prognosis and with expression of Bcl-2 and CD34 in de novo acute myeloid leukemia  
618 (AML): results from a multicenter trial of the Swiss Group for Clinical Cancer  
619 Research (SAKK). *Leukemia*. 1999;13(9):1352-1358.
- 620 47. Bencharit S, Cui CB, Siddiqui A, et al. Structural insights into fibronectin type  
621 III domain-mediated signaling. *J Mol Biol*. 2007;367(2):303-309.
- 622 48. Chi-Rosso G, Gotwals PJ, Yang J, et al. Fibronectin type III repeats mediate  
623 RGD-independent adhesion and signaling through activated beta1 integrins. *J Biol*  
624 *Chem*. 1997;272(50):31447-31452.
- 625 49. Korshunov VA. Axl-dependent signalling: a clinical update. *Clin Sci (Lond)*.  
626 2012;122(8):361-368.
- 627 50. Group PTC, Calabrese C, Davidson NR, et al. Genomic basis for RNA  
628 alterations in cancer. *Nature*. 2020;578(7793):129-136.
- 629 51. Zahn M, Marienfeld R, Melzner I, et al. A novel PTPN1 splice variant  
630 upregulates JAK/STAT activity in classical Hodgkin lymphoma cells. *Blood*.  
631 2017;129(11):1480-1490.
- 632 52. Zhou Y, Han C, Wang E, et al. Posttranslational Regulation of the Exon  
633 Skipping Machinery Controls Aberrant Splicing in Leukemia. *Cancer Discov*. 2020.
- 634 53. Dufies M, Jacquelin A, Belhacene N, et al. Mechanisms of AXL overexpression  
635 and function in Imatinib-resistant chronic myeloid leukemia cells. *Oncotarget*.  
636 2011;2(11):874-885.
- 637 54. Gioia R, Tregoeat C, Dumas PY, et al. CBL controls a tyrosine kinase network  
638 involving AXL, SYK and LYN in nilotinib-resistant chronic myeloid leukaemia. *J*  
639 *Pathol*. 2015;237(1):14-24.
- 640 55. Papadakis ES, Cichon MA, Vyas JJ, et al. Axl promotes cutaneous squamous  
641 cell carcinoma survival through negative regulation of pro-apoptotic Bcl-2 family  
642 members. *J Invest Dermatol*. 2011;131(2):509-517.
- 643 56. Zhao BS, Roundtree IA, He C. Post-transcriptional gene regulation by mRNA  
644 modifications. *Nat Rev Mol Cell Biol*. 2017;18(1):31-42.

- 645 57. Mandegar MA, Huebsch N, Frolov EB, et al. CRISPR Interference Efficiently  
 646 Induces Specific and Reversible Gene Silencing in Human iPSCs. *Cell Stem Cell*.  
 647 2016;18(4):541-553.
- 648 58. Aubrey BJ, Kelly GL, Kueh AJ, et al. An inducible lentiviral guide RNA  
 649 platform enables the identification of tumor-essential genes and tumor-promoting  
 650 mutations in vivo. *Cell Rep*. 2015;10(8):1422-1432.
- 651 59. Tam CS, Anderson MA, Pott C, et al. Ibrutinib plus Venetoclax for the  
 652 Treatment of Mantle-Cell Lymphoma. *N Engl J Med*. 2018;378(13):1211-1223.
- 653 60. Wang ML, Jurczak W, Jerkeman M, et al. Ibrutinib plus Bendamustine and  
 654 Rituximab in Untreated Mantle-Cell Lymphoma. *N Engl J Med*. 2022;386(26):2482-  
 655 2494.

## 656 **Figures Legends**

657

### 658 **Figure 1. MCL cells overexpress a new AXL isoform.**

659 **(A)** Schematic representation of AXL mRNA structure. The different set of primers  
 660 used for AXL mRNA amplification (RT-PCR) are indicated in purple (specific  
 661 amplification of isoform 1), green (amplification of isoform 1 and 2), and blue  
 662 (specific amplification of isoform 3). The new AXL 3 isoform (Bottom) is missing the  
 663 first four coding exons of the AXL isoform 1 and 2. **(B)** Relative mRNA expression of  
 664 the different AXL transcripts investigated by RT-PCR in MCL cell lines. All the  
 665 different AXL mRNA isoforms can be detected in MCL cells. MIA-PaCa-2 and K562  
 666 were used as positive controls for AXL amplification. **(C)** Detection of AXL protein  
 667 expression in MCL using an antibody targeting the N-terminal or **(D)** C-terminal  
 668 domain of AXL. The C-terminal antibody is able to recognize all AXL isoforms. The  
 669 AXL N-terminal antibody recognizes the isoform 1 and 2 but not the AXL3 isoform  
 670 since the antibody epitope is not present in AXL3. K562 and MIA-PaCa-2 served as  
 671 positive controls. **(E)** AXL can be detected at the cell surface of MCL cells by flow  
 672 cytometry staining using the AXL N-ter antibody. K562 served as a positive control.  
 673 Experiments were performed in triplicate. **(F)** AXL mRNA expression was  
 674 investigated by RT-PCR in primary MCL cells. All the AXL isoforms were expressed  
 675 in MCL primary cells. K562 and MIA-PaCa-2 served as positive controls for the AXL  
 676 1 and 2. **(G)** and **(H)** AXL is expressed at the protein level in MCL cells. AXL is  
 677 overexpressed in MCL cells in comparison to PBMCs or CD19<sup>+</sup> B-cells. **(I)** AXL 3 full  
 678 transcript was cloned and sequenced **(J and K)** and corresponds to the predicted  
 679 AXL3 isoform.

680

### 681 **Figure 2. AXL is constitutively activated in MCL cell lines and patient cells.**

682 (A) Western blot studies demonstrated the phosphorylation of AXL in all MCL cell  
683 lines. (B) JeKo-1 cells were treated with bemcentinib at concentrations ranging from  
684 0,5 to 4  $\mu$ M. Phosphorylation of AXL was evaluated using a p-AXL antibody.  
685 bemcentinib treatment reduces the level of AXL phosphorylation in MCL cells. (C)  
686 AXL phosphorylation status was evaluated in MCL patient cells by western blot. The  
687 AXL phosphorylation was detectable in all MCL patient cells. The results also  
688 indicated that AXL3 is the isoform predominantly activated in primary MCL cells. In  
689 contrast, CD19<sup>+</sup> B-cells from healthy individuals present a weak AXL activation and  
690 the complete absence of AXL3 phosphorylation. Experiments were performed in  
691 triplicate.

692

693

694 **Figure 3. Bemcentinib inhibits cell growth and induces cell cycle arrest and**  
695 **apoptosis of MCL cells.**

696 (A, B, C and D) MCL cell lines were treated with the AXL inhibitor bemcentinib in  
697 concentrations ranging from 0 to 8  $\mu$ M. The number of viable cells, as determined by  
698 trypan blue exclusion, decreased in a time and dose-dependent manner.  
699 Experiments were performed in triplicates and the means +/- standard deviations are  
700 shown. (E) Cell cycle analysis performed by flow cytometry revealed that AXL  
701 activity inhibition induces a cell cycle arrest of MCL cells. Triplicate experiments were  
702 performed and a representative result for each MCL cell lines is shown. (F and G)  
703 The JeKo-1 and Granta-519 MCL cell lines were treated with different concentrations  
704 of bemcentinib. The number of dead cells was assessed by trypan blue exclusion.  
705 Bemcentinib treatment induced cell death in a dose-dependant manner. The  
706 experiments were performed in triplicates and the means +/- standard deviations are  
707 shown. (H) Apoptosis was monitored by caspase activation in MCL cells (Mino,  
708 JeKo-1 and REC-1) treated with bemcentinib. Inhibition of AXL activity triggered  
709 apoptosis as revealed by PARP cleavage and caspase 3, 7 and 9 activations. (J)  
710 AXL inhibition by bemcentinib decreased NF- $\kappa$ B activation in MCL cell lines. NF- $\kappa$ B  
711 activation was evaluated by western blot using a phospho-antibody. Quantification of  
712 NF- $\kappa$ B activation is shown for each MCL cell lines. The experiments were performed  
713 in triplicates and the means +/- standard deviations are shown. (K) The expression  
714 of  $\beta$ -catenin, Cyclin D1, p-27 and GLUT-3 was investigated by western blot in JeKo-1

715 and REC-1 MCL cells. Bemcentinib treatment induced a dose-dependent decrease  
716 in  $\beta$ -catenin, Cyclin D1 and p-27 expression. No decrease in GLUT3 was observed.  
717 The experiments were performed in triplicates and a representative blot is shown for  
718 each cell line.

719

720 **Figure 4. AXL 3 knockdown induce apoptosis of MCL cells.**

721 (A) K562 and (C) JeKo-1 cells were transduced with a doxycycline inducible shAXL  
722 construct to block AXL expression. K562 and JeKo-1 control vector and shAXL cells  
723 were treated with an increasing dose of doxycycline for 96 hours. (B and D)  
724 Quantification of AXL expression by western blot after doxycycline treatment. (E)  
725 Quantification of cell number after doxycycline induction of shAXL. No effect on cell  
726 proliferation was observed for the control and shAXL cells. Experiments were  
727 performed in triplicate and the means +/- standard deviations are shown. (F)  
728 Apoptosis on JeKo-1 shAXL or K562 shAXL cells was evaluated by annexin V/PI  
729 staining after 96 hours of doxycycline treatment. Experiments were performed in  
730 triplicates, and a representative flow chart is shown. (G) JeKo-1 cells were  
731 transfected with AXL3 siRNA and AXL protein expression was assessed by western  
732 blot (left). Quantification studies (right) showed that AXL expression was decreased  
733 in MCL after treatment with AXL siRNA as compared to cells treated with scrambled  
734 siRNA ( $p < 0.003$ ). Experiments were performed in triplicates and the means +/-  
735 standard deviations are shown. (H) Treatment of the JeKo-1 MCL cell line with  
736 AXL siRNA significantly decreased the number of cells in comparison to cells treated  
737 with scrambled siRNA, as assessed by using the MTS assay ( $p < 0.0254$ ) and (I) cell  
738 counting, the differences were statistically significant ( $p < 0.0122$ ). (J) JeKo-1 cells  
739 were treated with scrambled or AXL3 siRNA and cell death was determined by  
740 trypan blue assay ( $p < 0.021$ ). (K) The morphological changes were examined by light  
741 microscopy. Scale bar= 100  $\mu$ M. Cell shrinkage and formation of apoptotic bodies  
742 were considered as apoptotic cells (Magnification $\times$ 200). (L) Using western blot,  
743 cleaved PARP was detectable in JeKo-1 cells treated with AXL3 siRNA.  
744 Quantification of PARP cleavage after AXL3 siRNA treatment (bottom). (M)  
745 Nucleolar morphological changes were observed under a fluorescence microscope  
746 after Hoechst-33342 staining. Scale bar= 20  $\mu$ M. Condensed or fragmented nuclei  
747 were considered as apoptotic cells ( $\times$ 400). Arrows indicate apoptotic cells. (N) AXL3



748 expression was downregulated using a CRISPRi method. sgRNAs targeting the  
749 AXL3 promoter were design to be induced by doxycycline treatment. Effect on AXL3  
750 protein expression was monitored by western blot. Quantification of AXL3 expression  
751 in comparison to control cells. Experiments were performed in triplicates and the  
752 means +/- standard deviations are shown. (O) Effect of AXL3 CRISPRi on cell  
753 proliferation was determined by cell counting. Experiments were performed in  
754 triplicates and the means +/- standard deviations are shown.

755

756 **Figure 5. Bemcentinib induces apoptosis of MCL primary cells. (A)** MCL patient  
757 cells were treated with DMSO or various concentrations of bemcentinib (0 to 8  $\mu$ M)  
758 for 24 hours. Relevant microscopy pictures revealed the presence of apoptotic cells  
759 and a reduction of the cell populations. Scale bar= 100  $\mu$ M. (B, C, D, E and F) Cell  
760 proliferation and cell death were measured by cell counting and trypan blue  
761 staining. Experiments were performed 4 times and the mean and distribution are  
762 shown. (G) Cell death was also investigated by flow cytometry using Annexin V/PI  
763 staining in MCL patient cells. Bemcentinib induced apoptosis in primary MCL cells *in*  
764 *vitro*.

765

766 **Figure 6. Inhibition of AXL by Bemcentinib reduces tumour burden and**  
767 **increases survival in an MCL xenograft mouse model.**

768 (A) Female NSG mice were injected i.v. with  $5 \times 10^5$  JeKo-1<sup>Luc+</sup> cells. The mice were  
769 imaged weekly, both dorsally and ventrally (10 minutes after i.p. injection with 150  
770 mg/kg of 25 mg/mL D-luciferin). The mice were distributed in the following groups  
771 control (vehicle only q.d), bemcentinib treatment (50 mg/kg b.i.d.), ibrutinib treatment  
772 (25 mg/kg q.d.), and combination treatment (ibrutinib + bemcentinib) based on total  
773 bioluminescence. Following the assignment, there was no statistical difference  
774 between the groups ( $p > 0.99$ ; one-way ANOVA test). JeKo-1<sup>Luc+</sup> xenografts were  
775 treated for 4 weeks with vehicle q.d. (control), ibrutinib (25 mg/kg, q.d.), bemcentinib  
776 (50 mg/kg, b.i.d.) or the combination of ibrutinib and bemcentinib (same dose as  
777 single treatment) ( $n = 6$ ). (B) BLI was assessed weekly to monitor disease  
778 progression. (C) Quantification of BLI signal from the different treatment groups  
779 week 3 ( $n = 6$ ). Bemcentinib significantly reduced the BLI signal in comparison to the  
780 control group ( $p < 0.0004$ ) or to Ibrutinib single treatment ( $p < 0.0247$ ) (D) Kaplan-Meier

781 plots showing the effect of the different treatments on the survival of mice  
782 xenografted with MCL cells ( $n = 8$ ).

